1 D contaminant transport through unsaturated stratified media using EFGM

S. Rupali[*1] and Vishwas A. Sawant[2a]

[1]*Department of Civil Engineering, Dr. B R Ambedkar National Institute of Technology Jalandhar ,144011, India*
[2]*Department of Civil Engineering, Indian Institute of Technology Roorkee, 247667, India*

Abstract.   In the present study, analysis of contaminant transport through one dimensional unsaturated stratified media using element free Galerkin method has been presented. Element free Galerkin method is a meshfree method. A FORTRAN code has been developed for the same. The developed model is compared with the results available in the literature and are found in good agreement. Further a parametric study has been conducted to examine the effects of various parameters like velocity, dispersivity, retardation factor and effect of saturation on the contaminant flow. The results presented conclude that transport of contaminant is retarded in unsaturated zone in comparison with the saturated zone.

Keywords: air quality; genetic programming; pune city; spatio temporal modelling

1. Introduction

A significant role is played by water and solutes which are being transferred through unsaturated-saturated ground in the field of agriculture and environmental engineering. The presence of fertilizers and pesticides used in agriculture can easily contaminate the water in unsaturated region. Unsaturated zones behave as containers which are used for controlling waste storage and removal and contamination of groundwater occurs when water is introduced due to rain or irrigation. Unsaturated zones are quite vulnerable to contamination and it has a direct association to the groundwater, which makes it important to have a good understanding of the transport in unsaturated regions. The actual process of the travel and fate of contaminants can be understood clearly with the help of mathematical models and hence play a significant role in the examination of the movement of contaminants.

Movement of water and contaminant in the unsaturated soil is described by the Richard's equation, even though it encounters severe convergence problems due to its nonlinear nature. Advection-dispersion equation has been commonly used for observing contaminant transport in porous media, (Bear 1979; Bear and Cheng 2010). Several algorithm are available in the literature for development of mathematical solutions for advection dispersion equation, out of which most

---

∗Corresponding author, Assistant Professor, E-mail: satavalekarr@nitj.com
[a]Associate Professor, E-mail: sawntfce@iitr.ac.in

common methods are the finite layer method (Rowe and Booker 1984, Fityus *et al*. 1999), boundary element method (Leo and Booker 1999), finite difference (Chakraborty and Ghosh 2010, Zhang *et al*. 2012, Sharma *et al*. 2014) and finite element methods (Li *et al*. 1999, Diaw *et al*. 2001, Javadi *et al*. 2008, Nezhad *et al*. 2011, Nezhad *et al*. 2013, Patil and Chore 2014). These methods exhibit oscillations or numerical dispersions. Seriousness of these problems are observed more for problems which are dominant in advection and have smaller dispersivities. Numerical oscillations can be avoided by employing upstream weighting or by employing restrictions of spatial divisions by using Peclet number P_e and achieving restriction on time step using the Courant number C_r. Kumar and Dodagoudar (2008a) in their study have revealed that EFGM is independent of Peclet numbers and are a good solution for advective-dominant problems.

Recently developed meshfree methods aimed to eliminate mesh generation and acquire approximate solutions for governing equations in terms of nodes (Liu 2002, Liu *et al*. 2005). Most common and successful meshfree method is the element free Galerkin method (EFGM) and has been employed for solving boundary value problems related to various field of studies (Belytschko *et al*. 1994, Lu *et al*. 1994, Belytschko and Tabbara 1996, Dolbow and Belytschko 1998, Kumar *et al*. 2007, Kumar and Dodagoudar 2008a, b, Satavalekar and Sawant 2014, Rupali and Sawant 2016, Satavalekar and Sawant 2016). Researchers have also applied meshfree finite point method (Onate and Idelsohn 1998) and point collocation method (Mategaonkar and Eldho 2011, Thomas *et al*. 2013) for flow and transport related problems.

The objective of the present analysis is to develop a numerical model using the meshfree technique which can produce precise simulations for solute transport in 1-D unsaturated– saturated stratified porous media. The flow model is based on the advective-dispersive equation, and is solved by EFGM considering stratification. The correctness of the proposed model is examined by comparing results with the numerical results from the literature. A detailed parametric study is performed to observe the effect of stratification, velocity, dispersivity and retardation coefficient on the migration of contaminant.

2. Model

EFGM is a meshless method as it only uses only set of nodes to model the boundary and generate discrete equations. It employs the moving least squares (MLS) approximants formulated by Lancaster and Salkauskas (1981) to approximate the function $C(x)$ with $C^h(x)$ in which $C(x)$ is the contaminant concentration at x, where x is a position coordinate. To perform the numerical integration in the weak form a background mesh is generated. The shape functions do not satisfy the Kronecker delta criterion and hence the Lagrangian multiplier technique (Dolbow and Belytschko 1998) is used to enforce the Dirichlet boundary condition.

2.1 Moving least squares approximations

According to the moving least squares proposed by Lancaster and Salkauskas (1981), the approximation $C^h(x)$ of $C(x)$ is

$$C(\,x\,) \cong C^h(\,x\,) = \sum_{i=1}^{m} p_i(\,x\,)a_i(\,x\,) = P^T(\,x\,)a(\,x\,) \qquad \forall x \in \Omega \tag{1}$$

in which,

$$P^{T} = [1 \ x] \text{ and } a^{T}(x) = [a_0(x), a_1(x), a_2(x), \dots a_m(x)] \tag{2}$$

where, $p(x)$ is a monomial basis function and $a(x)$ is a vector of undetermined coefficients, whose values can vary according to the position of x in Ω and m is the order of the basis.

The discrete L_2 norm is given by

$$J = \sum_{I=1}^{n} w(x - x_I)[C_L^h(x_I, x) - C_I]^2 = \sum_{I=1}^{n} w(x - x_I)[P^T(x_I)a(x) - C_I]^2 \tag{3}$$

where, n is the number of nodes in neighbourhood of x for which weight function $w(x\text{-}x_I)$ is non-zero and C_I refers to nodal parameter of C at $x = x_I$

The minimization of J in Eq. (3) with respect to $a(x)$ leads to the following set of linear equations

$$A(x)\text{a}(x) = B(x)u \tag{4}$$

or

$$a(x) = A^{-1}(x)B(x)u \tag{5}$$

where

$$
\begin{aligned}
A &= \sum_{I=1}^{n} w(x - x_I)P(x_I)P^T(x) \\
&= w(x - x_I)\begin{bmatrix} 1 & x_I \\ x_I & x_I^2 \end{bmatrix} + w(x - x_2)\begin{bmatrix} 1 & x_2 \\ x_2 & x_2^2 \end{bmatrix} + w(x - x_I)\begin{bmatrix} 1 & x_3 \\ x_3 & x_3^2 \end{bmatrix} + \dots \dots w(x - x_I)\begin{bmatrix} 1 & x_n \\ x_n & x_n^2 \end{bmatrix}
\end{aligned}
\tag{6}
$$

$$B(x) = w(x - x_I)\begin{bmatrix} 1 \\ x_I \end{bmatrix} w(x - x_2)\begin{bmatrix} 1 \\ x_2 \end{bmatrix} w(x - x_3)\begin{bmatrix} 1 \\ x_3 \end{bmatrix} \dots w(x - x_n)\begin{bmatrix} 1 \\ x_n \end{bmatrix} \tag{7}$$

$$C^{T} = [C_1, C_2, \dots C_n] \tag{8}$$

By substituting Eq. (5) in Eq. (1), the MLS approximants can be defined in terms of shape function $\varphi_I(x)$ as

$$C^h(x) = \sum_{I=1}^{n} \varphi_I(x)C_I = \varphi(x)C \tag{9}$$

and

$$\phi_I(x) = \sum_{j=0}^{m} p_j(x)(A^{-1}(x)B(x))_{JI} = P^T A^{-1} B_I \tag{10}$$

in which, m is the order of polynomial p(x).

Derivative of shape function are obtained by

$$\varphi_{I,x} = (P^T A^{-1} B_I), x = P_{,x}^T A^{-1} B_I + P^T (A^{-1})_{,x} B_I + P^T A^{-1} B_{I,x} \tag{11}$$

in which, $B_{I,x}$ and $A^{-1}{}_{,x}$ are computed as

$$B_{I,x}(x) = \frac{dw}{dx}(x - x_I)p(x_I) \tag{12}$$

$$A^{-1}{}_{,x} = -A^{-1} A_{,x} A^{-1} \tag{13}$$

where,

$$A_{,x} = \sum_{I=1}^{n} \frac{dw}{dx}(x - x_I)\begin{bmatrix} 1 & x_I \\ x_I & x_I^2 \end{bmatrix} \tag{14}$$

EFGM shape functions do not satisfy the Kronecker delta criterion $\varphi_I(x_J) \neq \delta_{IJ}$. Therefore they are not interpolants, and the name approximants is used. For imposing essential boundary conditions Lagrangian multipliers are used (Belytschko *et al.* 1994)

2.2 Weight function description

An important ingredient in EFG method is the weight function used Eq. (14). The weight function is non-zero over a small neighbourhood of x_I, called support domains. The weight function should be smooth and continuous. The choice of weight function affects the approximation results. Most of the weight functions are expressed in terms of non-dimensional distance $r_i = |x - x_i| / (d_{max} S_{av})$, where, d_{max} is a scaling parameter which is typically 2.0-3.0 for static analysis. The distance S_{av} is determined by searching for enough neighbour nodes for A to be regular.

Present study considers quartic spline function which is zero for $r_i \geq 1$, and for $r_i < 1$ given by

$$w(x - x_I) = 1 - 6r_i^2 + 8r_i^3 - 3r_i^4 \tag{15}$$

The derivatives for weight function are as follows

$$\frac{dw}{dx}(x - x_I) = (-12r_i + 24r_i^2 - 12r_i^3)\, \text{sign(x-x}_I) \tag{16}$$

3. Discretization of governing equation

The one dimensional governing equation for the advection-dispersion migration in an unsaturated porous medium is as follows

$$\frac{\partial(R\theta C)}{\partial t} = \frac{\partial}{\partial x}\left(\theta D \frac{\partial C}{\partial x}\right) - \frac{\partial(uC)}{\partial x} \tag{17}$$

in which, D is the dispersion coefficient (L^2/T) and it is expressed as $D = \alpha v + D^*$ where D^* is the diffusion coefficient [$L^2 T^{-1}$], α is the dispersivity [L] and u is the Darcy velocity [LT^{-1}]. Retardation factor R is related to bulk density of soil matrix ρ_b (M/L^3), distribution coefficient K_d (L^3/M) and volumetric water content θ as $R = 1 + \rho K_d / \theta$

C is concentration [ML^{-3}], C_0 is the concentration of contaminant at the source [ML^{-3}] and g is the concentration gradient at the exit boundary respectively and Γ_S and Γ_E are the boundaries at the start and end where the source concentration and concentration gradient is provided.

Initial boundary condition

$$C(x,t) = C_0 \quad on \ \Gamma_s; \quad and \quad \frac{\partial C}{\partial x} n_s = g \quad on \ \Gamma_E \tag{18}$$

The hydrodynamic properties of the soil are described by the functions of van Genuchten model (1980)

$$S = \frac{(\theta - \theta_r)}{(\theta_s - \theta_r)} = \left[1 + (\varpi \, |h|)^\chi \right]^{(1-\chi)/\chi} \quad for \quad h \le 0$$
$$S = 1 \quad for \quad h > 0 \tag{19}$$

$$K = K_s (S)^{0.5} \left[1 - \left(1 - S^{\left(\frac{\chi}{-1+\chi}\right)} \right)^{(1-(1/\chi))} \right]^2 \quad for \ \chi > 1 \tag{20}$$

$$\frac{\partial \theta}{\partial x} = -\varpi \left(\chi - 1\right)(\theta_s - \theta_r) S^{\chi/(\chi-1)} \left(1 - S^{\chi/(\chi-1)}\right)^{(\chi-1)/\chi} \tag{21}$$

in which, θ_r is the residual volumetric water content and θ_s is the saturated volumetric water content, S is the degree of saturation, K is the hydraulic conductivity at pressure head h [LT^{-1}] and K_S is the hydraulic conductivity at saturation [LT^{-1}], ϖ [L^{-1}] and χ are the empirical constants used for the determination of the shape of the function.

The weighted integral form of the Eq. (17) is expressed as

$$\int_0^L C^T \left[\frac{\partial}{\partial x}\left(\theta D \frac{\partial C}{\partial x} \right) - \frac{\partial}{\partial x}(uC) - \frac{\partial}{\partial t}(R\theta C) \right] dx = 0 \tag{22}$$

$$\int_0^L C^T \frac{\partial}{\partial x}\left(\theta D \frac{\partial C}{\partial x} \right) dx - \int_0^L C^T \frac{\partial}{\partial x}(uC) dx - \int_0^L C^T \frac{\partial}{\partial t}(R\theta C) dx = 0 \tag{23}$$

Integrating by parts yield

$$C^T \theta D \frac{\partial C}{\partial x} n_s \bigg|_{\Gamma_E} - \int_0^L \left(\frac{\partial C^T}{\partial x} \right) \theta D \left(\frac{\partial C}{\partial x} \right) dx +$$
$$\int_0^L C^T \left(\frac{\partial \theta}{\partial x} \right) D \left(\frac{\partial C}{\partial x} \right) dx - \int_0^L C^T \frac{\partial}{\partial x}(uC) dx - \int_0^L C^T \frac{\partial}{\partial t}(R\theta C) dx = 0 \tag{24}$$

To enforce boundary condition

$$C^T \theta D \frac{\partial C}{\partial x} n_s \bigg|_{\Gamma_E} - \int_0^L \left(\frac{\partial C^T}{\partial x} \right) \theta D \left(\frac{\partial C}{\partial x} \right) dx + \int_0^L C^T \left(\frac{\partial \theta}{\partial x} \right) D \left(\frac{\partial C}{\partial x} \right) dx$$

$$- \int_0^L C^T \frac{\partial}{\partial x}(uC) dx - \int_0^L C^T \frac{\partial}{\partial t}(R\theta C) dx - \Xi^T (C - C_0) \big|_{\Gamma_S} - \Xi^T C \big|_{\Gamma_S} = 0 \tag{25}$$

where L is the length of the domain and Ξ is a Lagrange multiplier for enforcing the essential boundary conditions.

$$[K]\{C\} + [M]\{\dot{C}\} + [G]\{\Xi\} = \{Q\}$$
$$[G]\{\Xi\} = \{q\} \tag{26}$$

in which

$$K_{IJ} = \int_0^L \left[\varphi_{I,x}^T \theta D \varphi_{J,x} + \varphi_I^T u \varphi_{J,x} + \varphi_I^T D_x \left(-\varpi \left(\chi - 1 \right) (\theta_s - \theta_r) S^{\chi/(\chi-1)} \left(1 - S^{\chi/(\chi-1)} \right)^{(\chi-1)/\chi} \right) \varphi_{J,x} \right] dx$$
$$\tag{27}$$

$$M_{IJ} = \int_0^L \left[\varphi_I^T R \theta \varphi_J \right] dx \quad ; \quad G_{IJ} = \varphi_K \big|_{\Gamma_{SI}} ; \quad Q = \varphi_I \theta D g \big|_{\Gamma_E} ; \quad q_K = C_{0K}$$

Adopting Crank Nicolson time marching scheme

$$\begin{bmatrix} K & G \\ G^T & 0 \end{bmatrix} \begin{Bmatrix} C_n \\ \Xi \end{Bmatrix} = \begin{Bmatrix} f_n \\ q \end{Bmatrix} \text{ where } f_n = \left([M] - 0.5 * \Delta t [K] \right) \{C\}_{n-1} \tag{28}$$

4. Algorithm

Based on the above mathematical formulation following steps are considered in the algorithm.
1. Set up nodal points and background cells
2. Set parameters for material properties like residual porosity, dispersion, velocity, retardation factor for each background cell of a given layer (for stratified case)
3. Set up initial concentrations C_I
4. Set up integration points and Jacobian for each cell
5. Loop over integration points
i) Calculate weights at each node for given integration point x_G
ii) Calculate shape functions and derivatives at points x_G
iii) Assemble Stiffness matrix [K] and Mass matrix [M]
iv) Assemble G matrix at 1st integration point for 1D
6. Apply the Crank Nicolson time marching scheme on stiffness matrix [K] and mass matrix [M]
7. Assemble Global Stiffness matrix [K$_G$] by adding stiffness matrix [K] and [G] matrix and obtain inverse the global stiffness matrix [K$_G$]$^{-1}$
8. Construct q_K vector
9. Loop over time

a) Construct {f} vector as $\{f\} = \left([M] - 0.5\Delta t[K]\right)\{C\}_{i-1}$

b) Compute new concentrations {C_i} by multiplying $[K_G]^{-1}$ inverse and {f} vector.

c) Set {C_{i-1}} = {C_i} for next time step.

5. Model verification

The methodology proposed for contaminant transport through unsaturated case using EFGM is validated with homogeneous case given by Diaw *et al*. (2001). The material properties used for the analysis of the problem are presented in Table 1. To model domain, 51 nodes are employed. The size parameter D_{max} of support domain is taken as 1.25. Fig. 1 shows the variation of normalized concentration with distance at the last time step. It can be observed from Fig. 1, that the results are in fair agreement with the results from Diaw *et al*. (2001). The results are also compared with that of Kumar *et al*. (2007) and it can be observed that the results are in very good agreement with those of Kumar *et al*. (2007). The present study is extended for layered media considering two and three layered soils.

Table 1 Material properties for homogeneous media from Diaw *et al*. (2001)

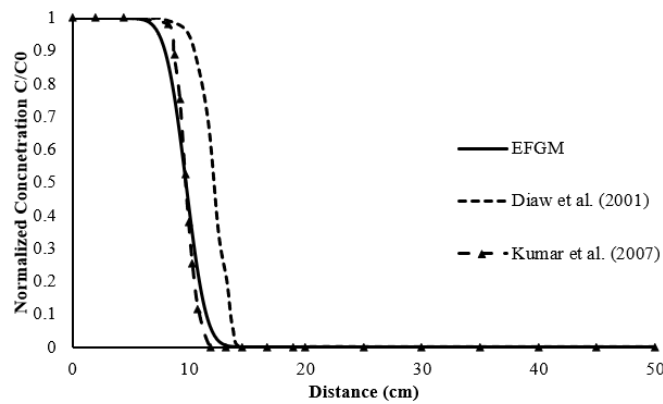| Parameter	Value
Length of domain (cm)	50
Saturated porosity θ_s	0.368
Residual porosity θ_r	0.102
Saturated hydraulic conductivity K_s(cm/s)	0.00922
Dispersivity α (cm)	0.1
Initial Pressure head h (cm)	-300
Boundary condition for flow at upper surface (cm)	-75
Boundary condition for flow at lower surface (cm)	-300
ϖ (cm^{-1})	0.0335
X	2.0
Time(hours)	12

Fig. 1 Comparison of EFGM with homogeneous strata from Diaw *et al*. (2001)

Table 2 Material properties for heterogeneous media from Diaw et al. (2001)

Parameter	Layer 1	Layer 2
Length of domain (cm)	20	20
Saturated porosity θ_s	0.3658	0.4686
Residual porosity θ_r	0.0286	0.106
Saturated hydraulic conductivity K_s(cm/day)	541	13.1
Dispersivity α (cm)	1.0	0.1
Initial Pressure head h (cm)	-1000	-1000
ϖ (cm^{-1})	0.028	0.0104
χ	2.239	1.1394
Time(days)	5	
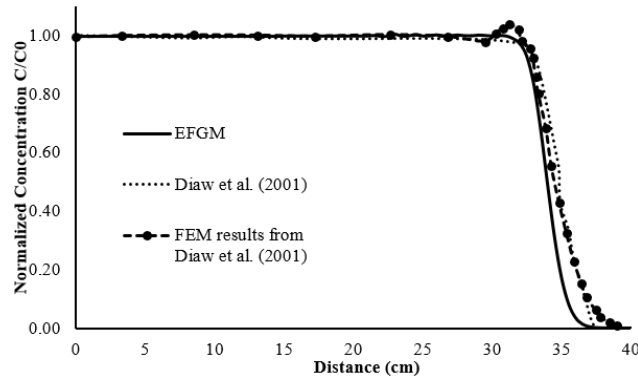
Fig. 2 Comparison of EFGM with layered strata from Diaw *et al*. (2001)

The methodology is extended for heterogeneous case given by Diaw *et al*. (2001). The two soils used were Berino loamy sand and Glendale Clay loam whose properties are reported in Table 2. Total of 81 nodes are used and size parameter D_{max} of support domain is 1.25 for the heterogeneous case. Variation of normalized concentration with distance at the last time step is presented in Fig. 2. It is observed from Fig. 2, that the results for stratified case are in good agreement with the results from Diaw *et al*. (2001). The results are also compared with FEM results presented in the literature (Diaw *et al*. 2001). It can be observed that meshfree results are in better agreement than those of FEM results. Similar results were reported by Kumar and Dodagoudar (2008a) for saturated case. Meshfree modelling is an effective tool when it comes to modelling advection dominated flow problems and this is evident from Kumar and Dodagoudar (2008a). The model is stable with any geometry and also good results are obtained using fewer nodes. This makes it an efficient tool for modelling contaminant transport. Study reported for saturated case (Satavalekar and Sawant 2016) demonstrated the effectiveness of meshfree analysis. The numerical model is further extended for unsaturated case.

6. Parametric study

A detailed parametric study considering the effect of velocity, retardation coefficient dispersivity and

Table 3 Material properties for sand-silt-clay layers

Parameter	Sand	Silt	Clay
Length of domain (cm)	20	20	20
Saturated porosity θ_s	0.372	0.396	0.446
Residual porosity θ_r	0.0388	0.131	0
Saturated hydraulic conductivity K_s (cm/day)	501.083	4.96	0.082
Dispersivity α (cm)	1.0	1.0	1.0
Initial Pressure head h (cm)		-1000	
ϖ (cm^{-1})	0.0437	0.00423	0.00152
X	1.8178	2.06	1.17
Time(days)		100	
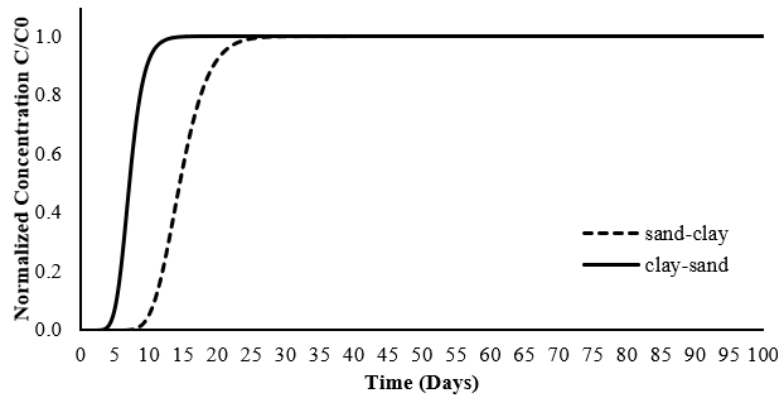
Fig. 3 Effect of sand and clay on the normalized concentration

degree of saturation is performed. The material properties reported in Table 3 for parametric study are selected from Saifadeen and Gladneyva (2012). Schematic representation of 1D geometry has been presented in Fig. 3. While examining effect of a particular parameter, only that particular parameter is varied in the selected range and other parameters are kept constant as reported in Table 3.

6.1 Effect of velocity

The contaminant travels with the velocity of the groundwater and is responsible for either accelerating or decelerating the contaminant migration. The influence of velocity is observed by considering three different soils with different hydraulic conductivity (sand, silt and clay) overlying one another. The normalized concentration at last node (60 m) function of time is presented in Fig. 4. It is observed that when sand is overlying clay, the normalized concentration of 0.9 is achieved at 20 days and thereafter remain constant till the last time step (total time 100 days). In case of clay overlying sand, the normalized concentration of 0.9 is achieved in 10 days and the concentration is constant till the last time step of 100 days.

Clay has very low permeability as compared to sand. By virtue of which, it is efficient in retarding the concentration. In general, presence of clay in top layers results in reduction of concentration. However, it is observed that more time is taken to reach 90% concentration when clay is underlying sand. This is due to consideration of small time span of 100 days. Early breakthrough is achieved in sand as compared to other soils. For effective reduction of concentration larger depth of clay layer should be present either overlying or underlying the sand.
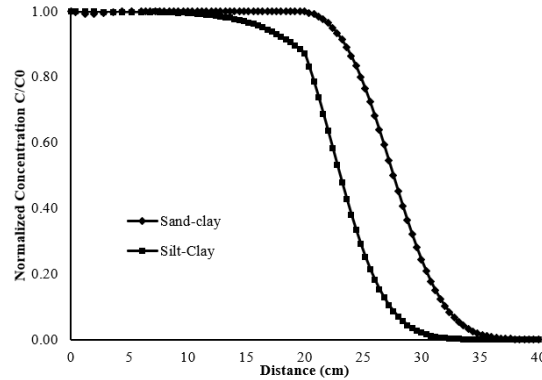
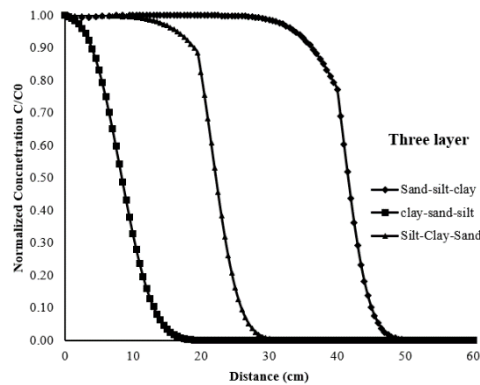Fig. 4 Effect of clay-silt and sand on the normalized concentration

Fig. 5 Effect of three layers on the normalized concentration

Another example of two different combination of soils viz. sand-clay and silt-clay are considered and the variation of concentration with distance for last time step is presented in Fig. 5. It is observed from Fig. 5 that solute transport is faster in sand-clay medium than in silt-clay medium. As compared to sand-clay, solute transport in silt-clay is lower because the permeability of sand is much higher than that of silt and clay.

Variation of concentration with distance considering combination of three soils has been presented in Fig. 6. It is observed that for clay-sand-silt arrangement (at last time step) reduction of concentration occurs immediately and is reduced to zero at 17cm depth, whereas reduction of concentration happens gradually due to the presence of sand and silt in the upper layers and concentration is reduced to zero at a distance of 30 cm and 50 cm for silt-clay-sand and sand-silt-clay (results for the last time step), respectively. From Fig. 8(a)-8(c) it can be observed that time taken to reach 90% concentration is more for sand-silt-clay (187days) than clay-silt-sand (175days) and silt-clay-sand (175days) (results are taken at last node). This concludes that for sand-silt-clay time taken is more because clay is in the bottom layer, whereas clay is present in top and middle layer in clay-silt-sand and silt-clay-sand case, presence of sand in the bottom layer will accelerate transport of contaminant.

For better understanding of arrangements of layer on transport of contaminant, a time versus distance graphs has been presented in Fig. 7. From Fig. 7(a) it can be observed that to achieve 90% concentration at a depth of 5cm it takes just 8 days when sand is at top whereas from Fig. 7(c) it can be observed that to achieve the same 90% concentration at a depth of 5cm it takes 52 days when clay is at the top layers. This explains that for determining achievement of a particular level of concentration at a particular depth and time can be obtained using these graphs. These graphs can be used for designing landfills or earthen barriers
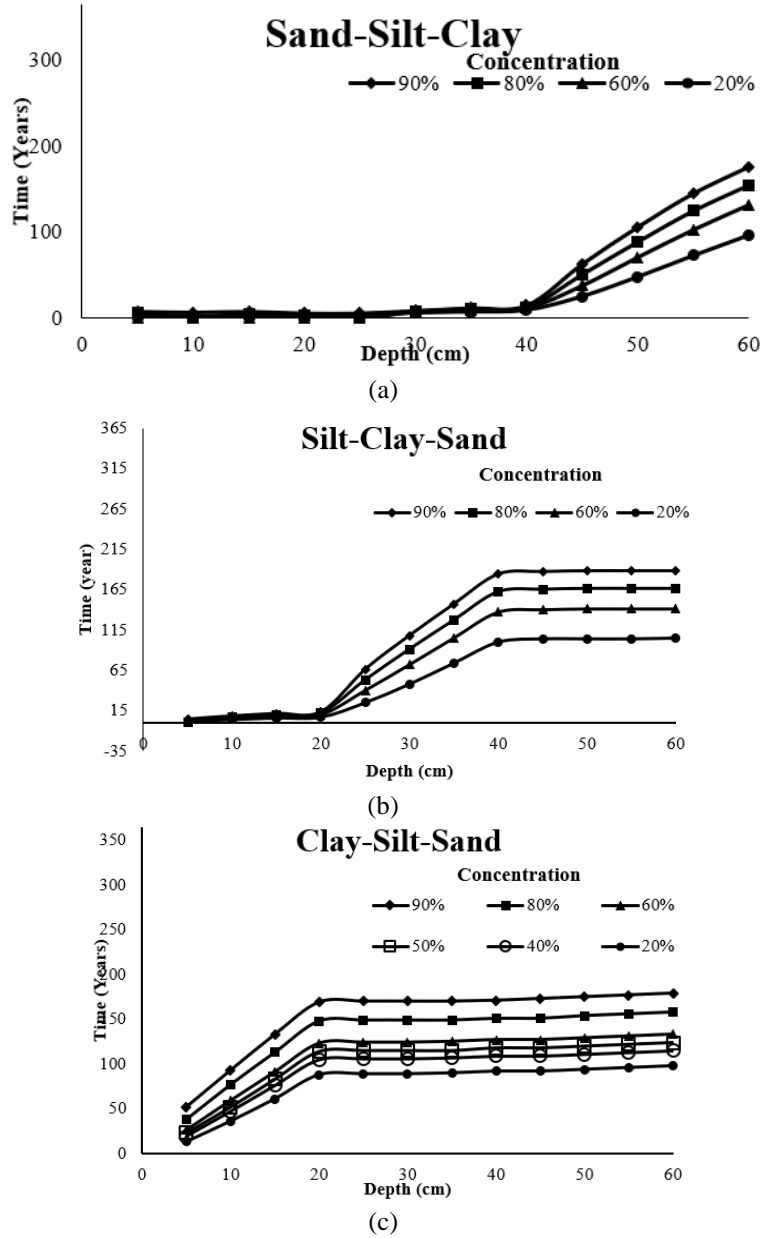
(a)

(b)

(c)

Fig. 6 Variation of time versus depth for various concentration

where judgement of concentration at a particular depth and time can be done and which can be used for determining the depth of a particular layer. Similar results were presented by Chakraborty and Ghosh (2011). In their study, effect of liner thickness on concentration level was discussed for different ions and compounds in saturated and homogeneous conditions.

Effect of velocity on normalized concentration in saturated and unsaturated regions is compared in Fig. 8. It is observed that time taken in the unsaturated zone is more than the saturated zone to reach one particular normalized concentration. From Fig. 8(a) it is noticed that it takes 187 days in unsaturated zone

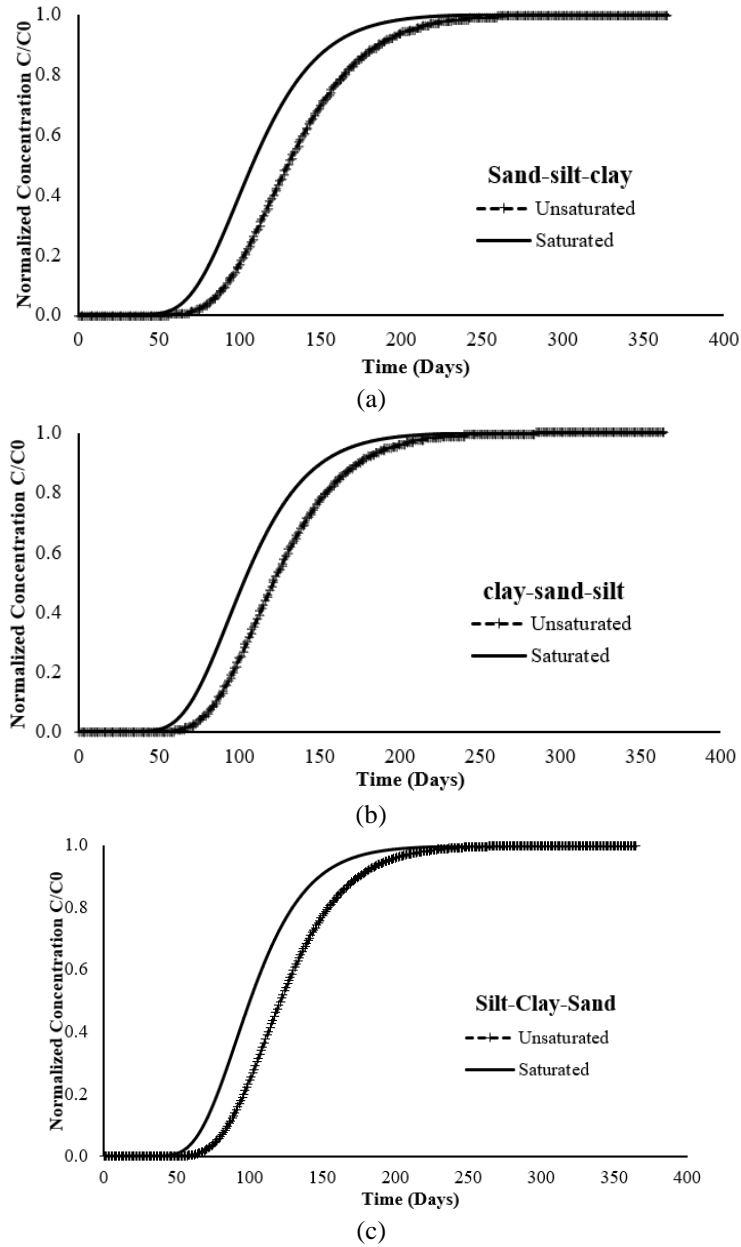*S. Rupali and Vishwas A. Sawant*

Fig. 7 Effect of velocity on saturated and unsaturated zone

and 159 days in saturated zone for Sand-silt-clay arrangement to reach the normalized concentration of 0.9 and it is nearly constant till the last time step. In Fig. 8(b) it is observed that it takes 175 days in unsaturated zone and 152 days in saturated zone for Clay-Silt-Sand arrangement to reach the normalized concentration of 0.9 and further it is more or less constant. From Fig. 8(c) it is observed that it takes 175 days in unsaturated zone and 148 days in saturated zone for Silt-Clay-Sand arrangement to reach the normalized concentration of 0.9 and further it is more or less constant. It is evident that transport of contaminant is retarded in case of unsaturated soil. Water content in the unsaturated layer is low compared to the saturated
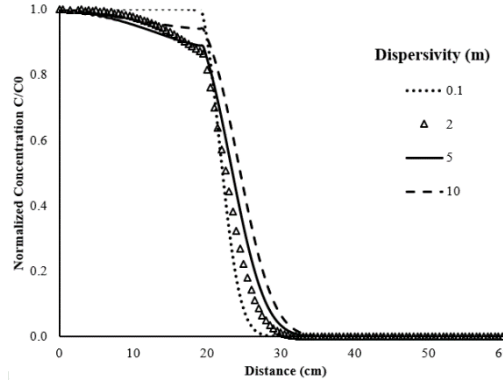
Fig. 8 Effect of dispersivity on normalized concentration in unsaturated media

layer leading to tortuous path and hence retarding the flow in unsaturated layers. Similar results were reported by Rowe and Badv (1996). They also observed that time taken by ions to migrate in saturated media was lesser than that in unsaturated media.

6.2 Effect of dispersivity

Dispersion is the product of mixing and spreading of the contaminant in the subsurface region. Dispersion is attributed to mechanical mixing and molecular diffusion. The mechanical dispersion is mixing component, which is defined by the product of the Darcy velocity in porous media and dispersivity. Dispersivity ranges from 0.1 to 100 m and approximate value for dispersivity is 0.1 times the scale of test (Gelhar *et al*. 1992). Effect of dispersivity on the transport of contaminant in unsaturated conditions is discussed in this section. The dispersivity values are varied only in the sand and silt layers and are not varied in clay as advective transport in clay soil is very negligible. The material properties for three different soils are same as reported in Table 3. The effect of dispersivity on concentration is presented in Fig. 9 for the last time step. The effect is observed on three layered soil where the position of sand is on top followed by silt and clay. It is observed that when the dispersivity is smaller, the migration of contaminant is less as compared to that for larger dispersivity. Dispersion refers to the spreading and mixing of the plume about the advective front, caused by molecular diffusion, dispersivity and by the variations in velocity. Smaller dispersivity will spread less plume and vice versa. Usually in field experiments, larger dispersivities are observed when the travel of contaminant is longer (Rastogi 2007). Similar effect is observed for contaminant transport in saturated media (Sharma *et al*. 2014, Satavalekar and Sawant 2016). Both the authors observed that when dispersivity/dispersion coefficient was increased, migration of ions was reduced.

Table 4 Time to achieve 90% concentration

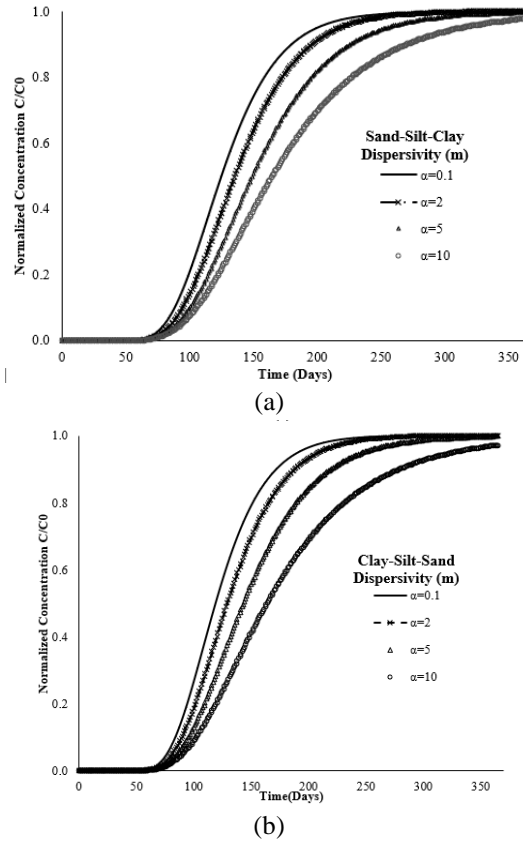| Dispersivity (m)	Unsaturated clay-silt-sand	Unsaturated sand-silt-clay	Saturated sand-silt-clay
0.1	170	180	159
2	185	195	159
5	220	225	159
10	280	270	159
15	335	302	159
20	381	322	159

(a)

(b)

Fig. 9 Effect of dispersivity on concentration in time domain

The effect of dispersivity on variation in normalized concentration in time domain is presented in Fig. 10. Fig. 10(a) presents the effect of dispersivity when the strata is arranged as sand, silt and clay and Fig. 10(b) presents the effect of dispersivity when the strata is arranged as clay, silt and sand. The results are plotted at a distance of 60 m. It is observed from the Fig. 10(a) (unsaturated sand-silt-clay) and Fig. 10(b) (unsaturated clay-silt-sand) that when dispersivity α is 0.1, normalized concentration of 0.9 is reached at the end of 180 days and 170 days, respectively. Time to achieve 90% concentration for different arrangements, is summarized in Table 4. With increase in dispersivity α, time to achieve 90% Concentration is increasing for both arrangements. With increase in dispersivity α from 0.1 to 20 m, time taken for sand-silt-clay arrangement is varying between 180 to 322 days, and corresponding time taken for clay-silt-sand arrangement is varying between 170 to 381 days. At smaller values of dispersivity α (0.1 to 5 m) time taken for 90% concentration in clay-silt-sand arrangement was lesser as compared to time in case of sand-silt-clay arrangements. But for dispersivity 10 m and higher, time taken in sand-silt-clay arrangements is lesser.

Effect of dispersivity on normalized concentration in saturated and unsaturated regions is compared in Fig. 11. It is observed that time taken in the unsaturated zone is more than the saturated zone to reach one particular normalized concentration. The results obtained are for sand-silt-clay arrangement. From Fig. 11(a) it is noticed that it takes 180 days in unsaturated zone and 159 days in saturated zone for the value of dispersivity equal to 0.1m to reach the normalized concentration of 0.9 and it is nearly constant till the last time step. Similar values for α = 2, 5, 10 m are reported in Table 4 (195, 225, 270 days for unsaturated case and 159 days for saturated case). It can be concluded that, dispersivity affects the contaminant transport in
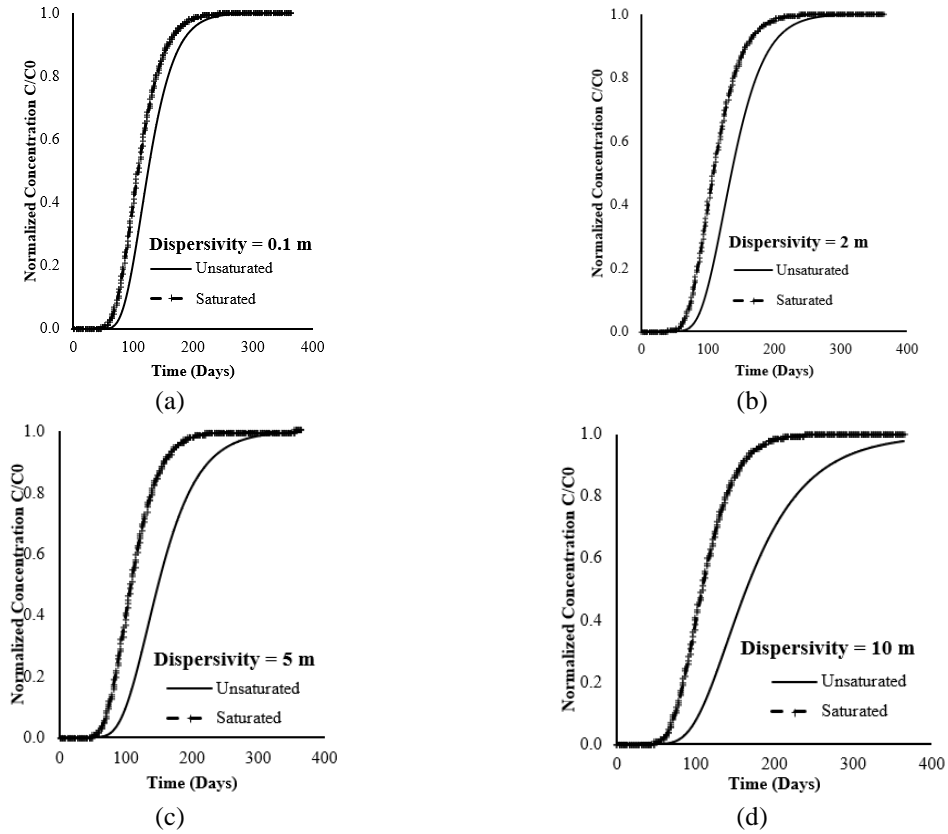
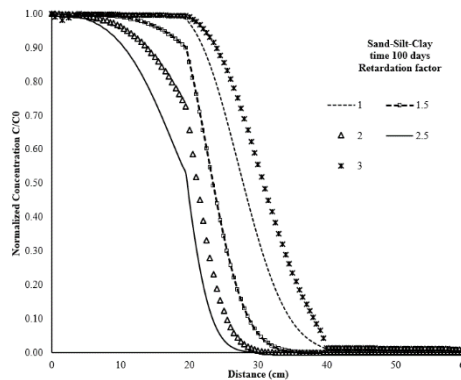Fig. 10 Effect of dispersivity on saturated and unsaturated zone

Fig. 11 Effect of Retardation factor on normalized concentration in unsaturated soil

unsaturated clay layers whereas the effect of dispersivity is not visible in saturated soils. Response for different values of dispersivity is same.

6.3 Effect of retardation factor

Retardation factor R comprises of porosity (n), distribution coefficient (K_d) and density (ρ) as $R = 1 + \rho$ K_d/ n. To study the effect, retardation factor R is varied between 1 to 3 at an interval of 0.5. The effect of
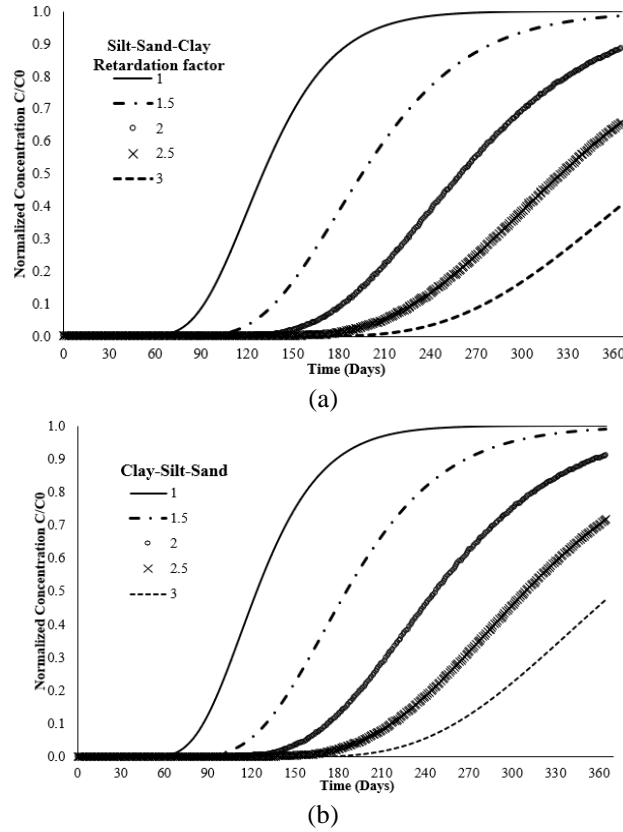
Fig. 12 Effect of retardation factor on concentration in time domain

retardation factor on normalized concentration in unsaturated zone is presented in Fig. 12 for last time step (total time 100 days). It is observed that the contaminant migration is retarded with an increase in retardation factor. Increase in retardation factor is due to increase in distribution coefficient K_d of the particular ion passing through the soil. This brings about adsorption/ion exchange at the soil and aqueous interface and ultimately resulting in reduction of normalized concentration. Similar effects are observed due to increase in retardation factor in saturated case as reported by Sharma *et al.* (2014) and Satavalekar and Sawant (2016).

The effect of retardation factor on variation in normalized concentration with time is presented in Fig. 13 (a) and (b). Fig. 13(a) presents the effect of retardation factor when the strata is arranged as sand, silt and clay and Fig. 13(b) presents the effect of retardation factor when the strata is arranged as clay, silt and sand. The results are plotted at a length of 60 m. It is observed from the Fig. 13(a) and (b) that normalized concentration of 0.9 is reached at the end of 187 days and 179 days when retardation factor is 1 for the cases of sand-silt-clay and clay-silt-sand. With increase in retardation factor time to achieve a specific level of concentration is increasing, as contaminant gets adsorbed on the soil leading to reduction in concentration.

When retardation factor is increased to 1.5, time taken to reach normalized concentration of 0.9 are 280 days and 275 days for sand-silt-clay arrangement and clay-silt-sand arrangement, respectively. Further increase in retardation factor to the value 2, 2.5 and 3 results in delay of contaminant transport. At the end of 365 days, the normalized concentration is reached to 0.88, 0.66 and 0.4 for sand-silt-clay arrangement and 0.91, 0.72 and 0.48 for clay-silt-sand arrangement.

Effect of retardation factor on normalized concentration in saturated and unsaturated regions is compared in Fig. 14 for sand-silt-clay arrangement. It is observed that time taken in the unsaturated zone is more than
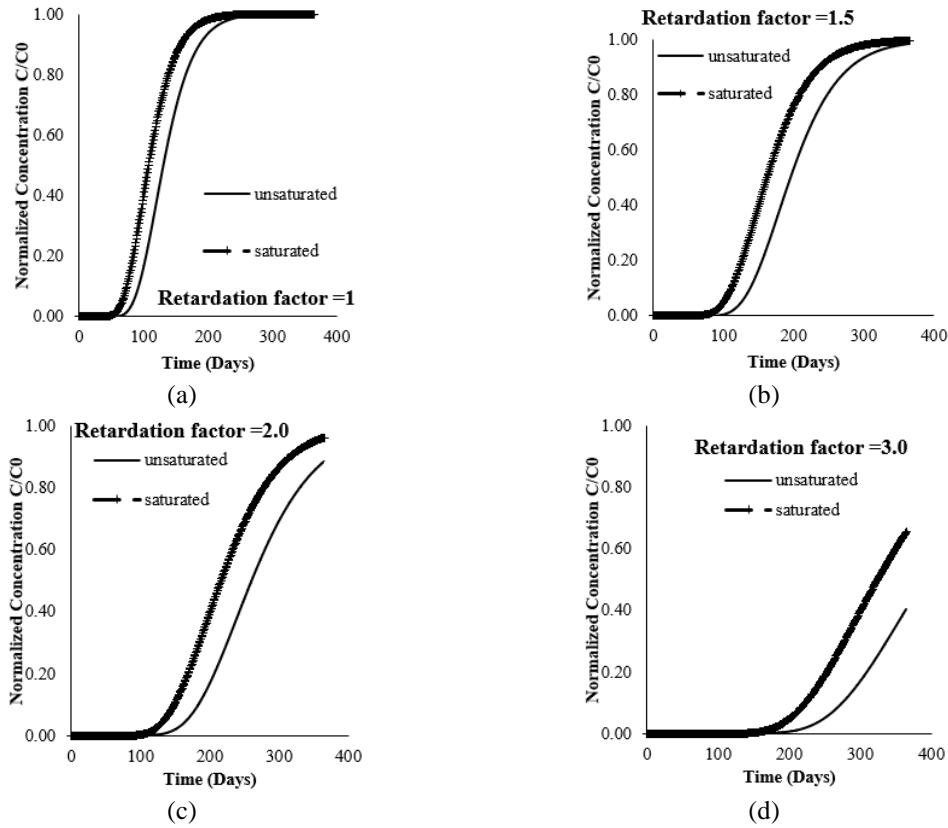
Fig. 13 Effect of retardation factor on saturated and unsaturated zone sand silt clay

the saturated zone to reach one particular normalized concentration. From Fig. 14(a) for $R = 1$, it is noticed that it takes 187 days in unsaturated zone and 159 days in saturated zone to reach the normalized concentration of 0.9 and it is nearly constant till the last time step. Similarly for $R = 1.5$, it requires 281 days in unsaturated zone and 238 days in saturated zone to reach the normalized concentration of 0.9 (Fig. 14(b)) and further it is more or less constant. For higher values of retardation factor R, it is observed that 90% concentration is not achieved within 365 days. After 365 days, concentration levels are 0.66 and 0.844 in unsaturated and saturated zone respectively for $R = 2$ (Fig. 14(c)). Corresponding concentration levels are 0.40 and 0.65 in unsaturated and saturated zone for $R = 3$ (Fig. 14(d)). It can be concluded that, effect of retardation factor is more prominent in unsaturated soils than in saturated soils.

6.4 Effect of saturation

Effect of saturation is incorporated by varying pressure head values. The different pressure head values are 1000 cm, 500 cm and 300 cm. The other material properties are the same as reported in Table 3. The layers are arranged as sand-silt-clay. The degree of saturation is calculated using the Eq. (19) and the different values for degree of saturation for the three different soils is reported in Table 5. Effect of degree of saturation as a consequence of different pressure head values is compared in Fig. 15 in the form of normalized concentration - distance relationship. It can be concluded that contaminant transportation increases with increase in degree of saturation. When the pressure head value is 1000 cm, the contaminant transported through different layers is lesser as compared to transport of contaminants occurring when

Table 1 Values of degree of saturation for different soils

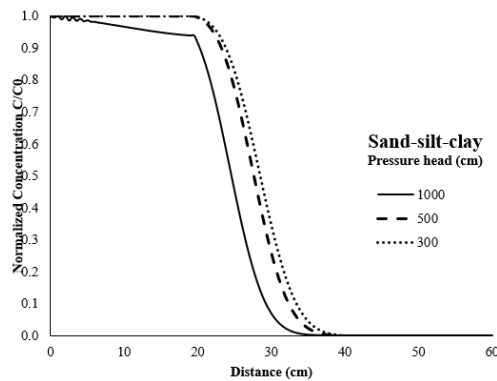| Suction head (cm)	Sand	Silt	Clay
1000	0.045521	0.211305	0.868819
500	0.080146	0.409153	0.923808
300	0.121399	0.607583	0.952384

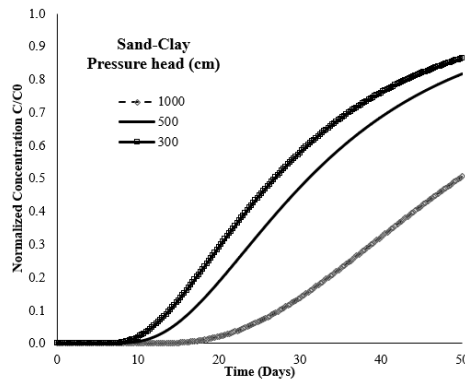Fig. 14 Effect of pressure head on normalized concentration

Fig. 15 Effect of pressure head on normalized concentration in time domain

pressure head values are 500 and 300 cm. Hence it is obvious that for larger pressure head values the transport of contaminants will be less in unsaturated soils.

Effect of pressure head on normalized concentration in time domain is presented in Fig. 16. It is observed from Fig. 16 that when the pressure head value is equal to 300 cm, the maximum normalized concentration reached is 0.86 at the end of 50 days. Similarly, the maximum normalized concentrations achieved after 50 days are 0.82 and 0.50 for pressure head value of 500 cm and 1000 cm, respectively. It can be concluded that pressure head values or degree of saturation affects the transport of contaminant in the unsaturated zones. Lower the saturation, lower is the contaminant transport and more is the time taken to reach the maximum normalized concentration.

In the unsaturated zone, the pore water is continuous or semi continuous and the pore water pressure are negative. The magnitude of the negative pore pressure (soil suction) is controlled by surface tension at the air-water boundaries within the pores and is governed by grain size. In general, the finer the soil particles,

the larger the saturation capillary head, and hence the higher the negative pore pressure. Rainfall infiltration from the ground surface may rapidly reduce the magnitude of negative pore pressure. Moreover, permeability decreases with decrease of degree of saturation. So contaminant transport phenomenon in unsaturated soil will not be exactly same as in case of saturated soil. It is more likely to take place at slower rate. Finer the soil, effect will be more.

7. Conclusions

Contaminant transport through unsaturated stratified media can be efficiently modelled using EFGM and it is verified with two examples from literature whose results are in good agreement. EFGM or meshfree model are efficient for problems concerning contaminant transport dominated by advection. Meshfree models are stable with any geometry and number of nodes. Parametric study is performed to observe the effect of change in velocity, dispersivity, retardation factor and degree of saturation. The arrangement of layers in unsaturated soils affect the contaminant migration and it is advisable to provide a clay layer on the top of a stratified containment to reduce the normalized concentration. Sand layer should be avoided as it will accelerate the transport of contaminants. Time taken for contaminant transport in unsaturated zone is more than in saturated zone and time taken for Sand-Silt-Clay arrangement among other layer arrangement is more. Time taken to reach maximum concentration is observed to be more for higher dispersivity values. The dispersivities of upper layers affect the contaminant transport in clay layers in unsaturated soils whereas the effect of dispersivity of upper layers is not visible in saturated soils. The contaminant migration is retarded with an increase in retardation factor. Lower the value of the retardation factor, more time is taken to reach a specific concentration level. Effect of saturation is observed by varying pressure head values. It can be concluded that pressure head values or degree of saturation affects the transport of contaminant in the unsaturated zones. Lower the saturation, lower is the contaminant transport and more is the time taken to reach the maximum normalized concentration. This is due to the presence of macropores, through which water and solutes may move preferentially, while bypassing a large part of the matrix pore-space.

References

Bear, J. (1979), *Hydraulics of Groundwater*. McGraw-Hill, New York, U.S.A.

Bear, J. and Cheng, A.H.D. (2010), *Modeling Groundwater Flow and Contaminant Transport*, Springer.

Belytschko, T. and Tabbara, M. (1996), "Dynamic fracture using element-free Galerkin methods", *Int. J. Numer. Meth. Eng.*, **39**(6), 923-938. https://doi.org/10.1002/(SICI)1097-0207(19960330)39:6%3C923::AID-NME887%3E3.0.CO;2-W.

Belytschko, T., Lu, Y.Y. and Gu, L. (1994), "Element-free Galerkin methods", *Int. J. Numer. Meth. Eng.*, **37**(2), 229-256.

Chakraborty, R. and Ghosh, A. (2010), "Finite difference method for computation of 1D pollutant migration through saturated homogeneous soil media", *Int. J. Geomech.*, **11**(1), 12-22. https://doi.org/10.1061/(ASCE)GM.1943-5622.0000068.

Diaw, E.B., Lehmann, F. and Ackerer, Ph. (2001), "One-dimensional simulation of solute transfer in saturated-unsaturated porous media using discontinuous finite elements method", *J. Contaminant Hydrol.*, **51**(3-4), 197-213. https://doi.org/10.1016/S0169-7722(01)00129-2.

Dolbow, J. and Belytschko, T. (1998), "An introduction to programming the meshless element free Galerkin method", *Arch. Comput. Meth. Eng.*, **5**(3), 207-241. https://doi.org/10.1007/BF02897874.

Fityus, S.G., Smith, D.W. and Booker, J.R. (1999), "Contaminant transport through an unsaturated soil liner beneath a landfill", *Can. Geotech. J.*, **36**(2), 330-354. https://doi.org/10.1139/t98-112.

Gelhar, L.W., Welty, C. and Rehfeldt, K.R. (1992), "A critical review of data on field-scale dispersion in aquifers", *Water Resour. Res.*, **28**(7), 1955-1974. https://doi.org/10.1029/92WR00607.

Javadi, A.A., Al-Najjar, M.M. and Evans, B. (2008), "Numerical modelling of contaminant transport through soils: Case study", *J. Geotech. Geoenviron. Eng.*, **134**(2), 214-230. https://doi.org/10.1061/(ASCE)1090-0241(2008)134:2(214).

Kumar, R.P. and Dodagoudar, G.R. (2008a), "Meshfree modelling of one-dimensional contaminant transport", *Geotechnique*, **58**(6), 523-526. https://doi.org/10.1680/geot.2008.58.6.523.

Kumar, R.P. and Dodagoudar, G.R. (2008b), "A 2D contaminant transport model for unsaturated soils", *Eng. Comput. Mech.*, **161**(3), 129-138.

Kumar, R.P., Dodagoudar, G.R. and Rao, B.N. (2007), "Meshfree modelling of one dimensional contaminant transport in unsaturated porous media", *Geomech. Geoeng.*, **2**(2), 129-136. https://doi.org/10.1080/17486020701379302.

Lancaster, P. and Salkauskas, K. (1981), "Surfaces generated by moving least-squares methods", *Math. Comput.*, **37**(155), 141-158. https://doi.org/10.1090/S0025-5718-1981-0616367-1.

Leo, C.J. and Booker, J.R. (1999), "A boundary element method for analysis of contaminant transport in porous media-II: Non-homogeneous porous media", *Int. J. Numer. Anal. Meth. Geomech.*, **23**(14), 1701-1715.
https://doi.org/10.1002/(SICI)1096-9853(19991210)23:14%3C1701::AID-NAG972%3E3.0.CO;2-W.

Li, X., Cescotto, S. and Thomas, H.R. (1999), "Finite-element method for contaminant transport in unsaturated soils", *J. Hydraul. Eng.*, **4**(3), 265-274. https://doi.org/10.1061/(ASCE)1084-0699(1999)4:3(265).

Liu, G.R. (2002), *Mesh Free Methods: Moving Beyond The Finite Element Method*, CRC Press, Boca Raton, Florida, U.S.A.

Liu, G.R. and Gu, Y.T. (2005), *An Introduction to Meshfree Methods and Their Programming*. Springer, Berlin, Germany.

Lu, Y.Y., Belytschko, T. and Gu, L. (1994), "A new implementation of the element-free Galerkin method", *Comput. Meth. Appl. Mech. Eng.*, **113**(3-4), 397-414. https://doi.org/10.1016/0045-7825(94)90056-6.

Mategaonkar, M. and Eldho, T.I. (2011), "Simulation of groundwater flow in unconfined aquifer using Meshfree point collocation method", *Eng. Anal. Boundary Elements*, **35**(4), 700-707. https://doi.org/10.1016/j.enganabound.2010.12.003.

Nezhad, M.M., Javadi, A.A. and Abbasi, F. (2011), "Stochastic finite element modelling of water flow in variably saturated heterogeneous soils", *Int. J. Numer. Anal. Meth. Geomech.*, **35**(12), 1389-1408. https://doi.org/10.1002/nag.966.

Nezhad, M.M., Javadi, A.A., Al-Tabbaa, A. and Abbasi, F. (2013), "Numerical study of soil heterogeneity effects on contaminant transport in unsaturated soil (model development and validation)", *Int. J. Numer. Anal. Meth. Geomech.*, **37**(3), 278-298. https://doi.org/10.1002/nag.1100.

Onate, E. and Idelsohn, S. (1998), "A mesh-free finite point method for advective-diffusive transport and fluid flow problems", *Comput. Mech.*, **21**(4-5), 283-292. https://doi.org/10.1007/s004660050304.

Patil, S.B. and Chore, H.S (2014), "Contaminant transport through porous media; An overview of experimental and numerical studies", *Adv. Environ. Res.*, **3**(1), 45-69. http://dx.doi.org/10.12989/aer.2014.3.1.045.

Rao, B.N. and Rahman, S. (2000), "An efficient meshless method for fracture analysis of cracks", *Comput. Mech.*, **26**(4), 398-408. https://doi.org/10.1007/s004660000189

Rastogi, A.K. (2007), *Numerical Groundwater Hydrology, Penram International Publishing (I) Pvt. Ltd.*, India.

Rowe, R.K. and Badv, K. (1996), "Advective-diffusive contaminant migration in unsaturated sand and gravel", *J. Geotech. Eng.*, **122**(12), 965-975. https://doi.org/10.1061/(ASCE)0733-9410(1996)122:12(965).

Rowe, R.K. and Booker, J.R. (1984), "The analysis of pollutant migration in a non-homogeneous soil",

Geotechnique, **34**(4), 601-612. https://doi.org/10.1680/geot.1984.34.4.601.

Rupali, S. and Sawant, V.A. (2016), "1 D contaminant transport using Element free Galerkin method with irregular nodes", *Coupled Syst. Mech.*, **5**(3), 203-221. https://doi.org/10.12989/csm.2016.5.3.203.

Saifadeen, A. and Gladneyva, R. (2012), "Modeling of solute transport in the unsaturated zone using Hydrus-1D", M.Sc. Dissertation, Lund University, Lund, Switzerland.

Satavalekar, R.S. and Sawant, V. A. (2014), "Numerical modelling of contaminant transport using FEM and meshfree methods", *Adv. Environ. Res.*, **3**(2), 117-129. http://dx.doi.org/10.12989/aer.2014.3.2.117.

Satavalekar, R.S. and Sawant, V.A. (2016), "Two dimensional contaminant transport through layered soil using element free galerkin method", *Indian Geotech. J.*, **46**(2), 192-205. https://doi.org/10.1007/s40098-015-0156-4.

Sharma, P.K., Sawant, V.A., Shukla, S.K. and Khan, Z. (2014), "Experimental and numerical simulation of contaminant transport through layered soil", *Int. J. Geotech. Eng.*, **8**(4), 345-351. https://doi.org/10.1179/1939787913Y.0000000014.

Thomas, A., Eldho, T.I. and Rastogi, A.K. (2013), "A comparative study of point collocation based meshfree and finite element methods for groundwater flow simulation", *ISH J. Hydraul. Eng.*, **20**(1), 65-74. https://doi.org/10.1080/09715010.2013.840120.

CC